Life Sciences 363 (2025) 123401

Contents lists available at ScienceDirect

Life Sciences

journal homepage: www.elsevier.com/locate/lifescie

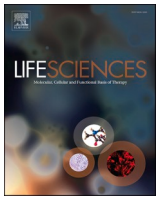

Pharmacologically induced proteolysis of histone deacetylase-6 attenuates influenza virus replication despite limited anti-tumor effects

Johannes Jungwirth [a,b,1], Andreas O. Mieland [b,1], Andrea Piée-Staffa [b], Tino Heimburg [c], Walburgis Brenner [d], Christina Ehrhardt [a], Wolfgang Sippl [c,*], Andreas Henke [a,*,2], Oliver H. Krämer [b,*,2]

[a] Section of Experimental Virology, Institute of Medical Microbiology, Center for Molecular Biomedicine (CMB), Jena University Hospital, Jena, Germany
[b] Department of Toxicology, University Medical Center of the Johannes Gutenberg University Mainz, Mainz, Germany
[c] Department of Medicinal Chemistry, Institute of Pharmacy, Martin-Luther-University of Halle-Wittenberg, Halle (Saale), Germany
[d] Department of Obstetrics and Gynecology, University Medical Center of the Johannes Gutenberg University Mainz, Mainz, Germany

ARTICLE INFO

Keywords:
HDAC6
Leukemia
PROTAC
Influenza virus
Lung cancer
CRBN

ABSTRACT

The protein deacetylase HDAC6 has been controversially linked to cancer cell proliferation and viral propagation. We analyzed whether a pharmacological depletion of HDAC6 with a recent proteolysis-targeting chimera (PROTAC) kills tumor cells. We show that low micromolar doses of the cereblon-based PROTAC TH170, but not its inactive analog TH170E, induce proteasomal degradation of HDAC6. The elimination of HDAC6 by TH170 does not compromise leukemia cell growth and survival, DNA integrity, and the stability of selected cancer-relevant proteins. Increasing the doses of TH170 generates a hook-effect on HDAC6 degradation and the apoptosis-associated fragmentation of HDAC6. Unlike the specific elimination of HDAC6 that low doses of TH170 evoke, this fragmentation of HDAC6 is linked to apoptosis and an accumulation of acetylated histones. Thus, like HDAC6 inhibitors, pharmacological degraders of HDAC6 do not induce leukemic cell death unless they are used in non-selective concentrations. Bioinformatic analyses of 91 lymphoid, 37 myeloid, and 125 lung cancer cells in which HDAC6 was deleted by CRISPR-Cas9 corroborate these data. HDAC6 is expressed in various bronchus and lung cell types. In a human lung cell model, TH170 reduces influenza A virus replication dependent on the strain and without compromising cell vitality. These data suggest that pharmacologically amenable kinase-independent functions of HDAC6 control viral replication. Eliminating HDAC6 could be a promising anti-viral strategy with a benign impact on host cells.

1. Introduction

Dysregulated protein acetylation is an increasingly appreciated marker of tumor development and progression. Protein deacetylases remove the acetylation mark from the ε-N lysine residue in proteins and thereby antagonize the biochemical activity of protein acetyl transferases. For historical reasons, these enzymes are called histone deacetylases (HDACs) and histone acetyltransferases (HATs), respectively. Small molecule inhibitors against HDACs are considered as clinically relevant compounds. These act against members of the 11 zinc-dependent HDACs, being divided into classes I, II, and IV [1,2].

The class IIB deacetylase HDAC6 resides mainly in the cytosol and has no detectable in vivo activity against histones. Therefore, HDAC6 is often referred to as protein deacetylase (PDAC) [3]. To maintain consistency, we keep the nomenclature as HDAC6.

Oncological relevant substrates of HDAC6, including the chaperone HSP90, suggested that HDAC6 was a valid anti-leukemic target [4,5]. However, increasing evidence accumulates that inhibition or genetic elimination of HDAC6 does not compromise the growth of most hematopoietic and solid tumor cells in vitro and in vivo [6–14]. Discrepant

* Corresponding authors.
E-mail addresses: johannes.jungwirth@med.uni-jena.de (J. Jungwirth), amieland@students.uni-mainz.de (A.O. Mieland), pieean01@uni-mainz.de (A. Piée-Staffa), brenner@uni-mainz.de (W. Brenner), christina.ehrhardt@med.uni-jena.de (C. Ehrhardt), wolfgang.sippl@pharmazie.uni-halle.de (W. Sippl), andreas.henke@med.uni-jena.de (A. Henke), okraemer@uni-mainz.de (O.H. Krämer).
[1] Equal first authors.
[2] Equal last authors.

https://doi.org/10.1016/j.lfs.2025.123401
Received 14 October 2024; Received in revised form 23 December 2024; Accepted 11 January 2025
Available online 13 January 2025

data on previously reported anti-cancer effects of HDAC6 inhibitors can be explained by the application of too high inhibitor concentrations that also inhibit class I HDACs. This compromises cell survival by mechanisms beyond HDAC6 inhibition. Notably, the lack of anti-proliferative effects of HDAC6 mirrors the full vitality of HDAC6 knock-out animals and the ample proliferation of cells from them [15].

Proteolysis-targeting chimeras (PROTACs) are innovative agents that are based on pharmacophore fusions of inhibitors, linkers, and ligands recruiting E3 ubiquitin ligases. For example, PROTACs containing immunomodulatory drugs (e.g., lenalidomide, thalidomide) recruit cereblon, an adapter for ubiquitin ligases, to eliminate proteins of interest. The E3 enzymes catalyze the transfer of K48-linked ubiquitin moieties to the proteins that are bound by the inhibitors. This leads to a degradation of their targets by the proteasome, an intracellular multiprotease complex, and the recycling of the drug for multiple degradation rounds [16].

Influenza A virus (IAV) belongs to the virus family of the *Orthomyxoviridae*. Infections with this pathogen have a tremendous medical impact worldwide. Caused by high mutation rates of the viral genome, established treatment options against IAV proteins are becoming less and less effective. Therefore, the search and development of new antiviral strategies against IAV-caused diseases, based on the detailed understanding of virus-host interactions is increasingly important. In this context, it was previously shown that HDAC6 activity is essential for successful viral replication [17]. During the IAV uncoating process, the viral ribonucleoprotein (vRNP) complex dissociates from viral M1 proteins. Hereby, the aggresome processing pathway (APP) is activated, which recruits molecular motor proteins like dynein and myosin-10 together with HDAC6 via its ubiquitin-binding zinc finger domain to viral M1 proteins. Due to the physical breaking of capsid structures, M1 is separated from vRNPs. This induces the transport of vRNPs into cellular nuclei. Single amino acid changes in the M1 protein of clinical IAV isolates influence its binding to HDAC6, which might be important for viral infectivity [18]. Based on multiscale kinetic models about the precise mechanism of the uncoating process, the development of drugs, like designed ankyrin repeat proteins (DARPins) to interfere with HDAC6 binding, paves the way to new anti-viral strategies by disrupting the HDAC6-ubiquitin interaction not only in case of IAV [19] but of Zika virus infections as well [20]. However, next to this proviral impact, HDAC6 exerts anti-viral effects that are linked to its enzymatic activity. Such effects are based on (I) decreased transport of viral components to the plasma membrane [21], (II) reduced viral budding by tubulin deacetylation [22], (III) deacetylating of cellular retinoic acid inducible gene I to promote viral RNA detection [23] together with enhanced release of anti-viral interferons and proinflammatory cytokines, and (IV) deacetylation of the IAV polymerase complex to restrict viral RNA transcription/replication [24]. These findings show that under certain experimental conditions HDAC6 carries out both anti- and pro-viral effects.

We asked whether an acute pharmacological reduction of HDAC6 with a cereblon-based HDAC6 PROTAC impaired the growth and survival of leukemic cells. We chose such cells because pan-HDACi are approved by food-and-drug administrations to treat certain blood cancers [1,2]. We demonstrate that the PROTAC TH170 induces a loss of HDAC6. Consistent with the data that were collected with HDAC6 inhibitors, a selective pharmacological degradation of HDAC6 exerts biochemical activity but does not kill leukemia cells. Higher doses of TH170 produce apoptosis-associated anti-leukemic effects that are associated with histone hyperacetylation as sign of class I HDAC inhibition. Since structural properties of HDAC6 were reported as determinants of the replication and spread of IAV, the influence of TH170 on IAV progeny production was analyzed in virus-infected human lung epithelial cells. In this regard, we report the first HDAC6 degrader with anti-viral activity.

2. Material and methods

2.1. Chemicals

The syntheses of the HDAC6 PROTAC TH170, its corresponding inhibitor TH137, and the negative control TH170E were recently described by us [25]. Entinostat MS-275 (S1053), MG-132 (S2619) and pomalidomide (S1567) were bought from Selleck chemicals and were dissolved in DMSO to a 1 mM stock. The compounds were further diluted in phosphate buffered saline (PBS) or the culture media to keep DMSO concentrations below 0.1 %.

2.2. Cell lines and viruses

The leukemia cell lines MOLM–13, MV4–11, RS4–11, Ramos (RA1, EBV-negative), and MOLT–4 were cultured in RPMI (Sigma R8758) plus 5–10 % FCS (Sigma Superior S0615). MOLT-4 cells with and without cereblon were kindly provided by Dr. Georg E. Winter, Vienna. Human epithelial lung cancer cells A549 (ATCC Cat. No. CCL-185) were cultivated in DMEM (Anprotec AC-LM-0012) plus 10 % FCS (Anprotec AC-SM-0190). The A549-HDAC6^{KO}, A549-HDAC6^{CDm} and A549-HDAC6^{Znf} cells were kindly provided by Prof. Dr. Patrick Matthias, Basel. These cells were grown in DMEM plus 10 % FCS. The IAV strains used in this work were the A(H1N1) Puerto Rico/8/34 (PR8) and the H1N1 pdm09 A/mpJena/5258/09 HA-222D/G (Jena/5258) from the 2009 pandemic outbreak in Jena, Germany [26], which were both propagated in Madin-Darby canine kidney cells (MDCK, ATCC Cat. No. CCL-34) and Panserin 401 (PAN Biotech P04–710401). Non-infected MDCK cells were cultivated in MEM (Anprotec AC-LM-0043) plus 10 % FCS (Anprotec AC-SM-0190). All cells were tested free of mycoplasma by enzymatic testing (MycoStrip, Invivogen, Toulouse France).

2.3. Viral infection and plaque assay

Per well, 10^6 A549 cells were seeded 24 h prior viral infection in 6-well plates. For the PROTAC testing the cells were pre-treated with substances for 12 h in DMEM for infection ($DMEM_{INF}$). This medium is DMEM with 0.2 % BSA (Roth 9401.3), 1 mM $MgCl_2$, 0.9 mM $CaCl_2$ and 100 U/ml penicillin, 0.1 mg/ml streptomycin (Anprotec AC-AB-0024). Cells were once washed with PBS before infection with a multiplicity of infection (MOI) of 1.0 IAV in PBS_{INF}. This is PBS with 0.2 % BSA, 1 mM $MgCl_2$, 0.9 mM $CaCl_2$, 0.17 μg/ml TPCK-treated trypsin (Sigma T-1426) and 100 U/ml penicillin, 0.1 mg/ml streptomycin for 60 min at 37 °C and 5 % CO_2. After aspiration of IAV, cells were incubated for additional 23 h in $DMEM_{INF}$ (supplemented with 0.17 μg/ml TPCK-treated trypsin) respectively with $DMEM_{INF}$ from the pre-treatment supplemented with 0.17 μg/ml TPCK-treated trypsin. Cell culture supernatants were used to determine progeny viral titers and cells were lysed for immunoblot analyses. Per well, 2×10^6 MDCK cells were seeded 24 h prior standard plaque assay in 6-well plates. Cells were infected with serial dilutions of viral-containing supernatants in PBS_{INF} for 30 min at 37 °C and 5 % CO_2. The PBS_{INF} was aspirated, and cells were incubated with plaque medium (MEM with 0.2 % BSA, 0.01 % DEAE-Dextran (Pharmacia Biotech 17-0350-01), 0.2 % $NaHCO_3$ (Anprotec AC-DS-0017), 100 U/ml penicillin, 0.1 mg/ml streptomycin and 0.25 μg/ml TPCK-treated trypsin) and 0.9 % agar (Thermo Scientific LP0028B) at 37 °C and 5 % CO_2 for three days. Plaques were visualized with crystal violet staining (water with 0.2 % crystal violet, 20 % ethanol and 3 % formaldehyde) and the number of plaques was counted.

2.4. Immunoblot and antibodies

We recently described this technique in [27]. All immunoblots are representative of at least two independent experiments and most

experiments were done in several cell lines.

antibody	source and catalogue number	dilution
HSP90	Santa Cruz sc13119	1:2000
β-actin	Santa Cruz sc47778	1:2000
vinculin	Santa Cruz sc736	1:2000
acetylated tubulin (ac-tubulin)	Sigma T7451	1:5000
tubulin-α	Abcam ab176560	1:500
acetylated histone H3 (ac-H3)	Millipore 06–599	1:1000
HDAC6	Cell Signaling 7558	1:625
FLT3	Cell Signaling 3462	1:500
HDAC1	Cell Signaling 34589S	1:500
HDAC10	Sigma H3413	1:1000
p53	Santa Cruz sc6243	1:2000
cleaved caspase-3	Cell Signaling 9661	1:500
cleaved PARP1	BD Pharmingen 552596	1:1000
MYC	Cell Signaling 5605	1:500
beclin-1	Cell Signaling 3495	1:1000
cereblon	Cell Signaling 71810	1:1000
RAD51	Abcam 63801	1:500
γH2AX	Cell Signaling 9718	1:1000
USP10	Abcam 109219	1:500

Cell proliferation analysis.

Cells were seeded at low densities, treated one day later with TH170 for 4–5 d, and counted with a hemocytometer.

2.5. MTT-test

To determine the cell metabolic activity upon treatment with the test compounds, 15,000 A549 cells in 100 μl DMEM were seeded per well 24 h prior use into 96-well plates and incubated at 37 °C and 5 % CO_2. Substance dilutions were prepared freshly in DMEM for each experiment. Cells were washed once with PBS. Afterwards, 100 μl of DMEM including the respective substances in the specified concentrations were added and cells were further incubated for 24 h at 37 °C and 5 % CO_2. Thereafter, 25 μl of 5 mg/ml MTT (Sigma Aldrich, M5655) was added and cells were incubated for another 2 h. Thereafter, supernatants were removed carefully and DMSO was added to lyse cells. Metabolic activity was determined via relative absorbance at the OD 562 nm compared to the untreated control using a FLUOstar Omega plate reader (BMG Labtech, Ortenberg, Germany).

2.6. Flow cytometry to assess apoptosis

Early apoptosis and late apoptosis/necrosis were assessed with annexin-V/propidium iodine (PI) staining followed by flow cytometry, as recently described by us in [28].

2.7. Global analyses and statistics

Data generated by DepMap are made available under the permissive CC BY 4.0 license (DepMap: The Cancer Dependency Map Project at Broad Institute). The Human Protein Atlas is licensed under the Creative Commons Attribution Share Alike 3.0 International License (The Human Protein Atlas). Statistical analyses were performed in GraphPad Prism 8, as described in the figure legends.

3. Results

3.1. The PROTAC TH170 eliminates HDAC6 dose-dependently

We have recently described the chemical synthesis of TH170 [25,29]. This agent consists of a hydroxamic acid moiety that can form a complex with the catalytically active Zn^{2+} in the catalytic pocket of HDACs, a linker, and a domain recruiting E3 ubiquitin ligase complexes containing cereblon. The chemical structure of TH170 is shown in Fig. 1a.

We analyzed the impact of TH170 on HDAC6 in MV4–11 cells (from a 10-year-old boy with acute myeloid leukemia, AML) and MOLM–13 cells (from a 20-year-old male with AML, evolved from myelodysplastic syndrome). Both cell lines carry clinically unfavorable internal tandem duplications in the feline McDonough sarcoma-related tyrosine kinase-3 (FLT3-ITD). We incubated these cells with 0.1 to 20 μM TH170 for 24 h. In MV4–11 and MOLM–13 cells, 0.5 μM TH170 reduced HDAC6 and caused an accumulation of acetylated tubulin. Increasing the concentrations of TH170 to 1 and 2 μM TH170 did not augment these effects (Fig. 1b). Pharmacodynamic markers for the inhibition of HDAC6 or class I HDACs (HDAC1/−2/−3/−8) are the accumulation of acetylated tubulin or acetylated histones, respectively [30]. The attenuation of HDAC6 and the accumulation of acetylated tubulin were not associated with an increase in acetylated histone H3 or an effect on the levels of the class I deacetylase HDAC1 in these cells (Fig. 1b).

Having verified the specificity of TH170 at up to 2 μM, we defined if lower concentrations of TH170 were effective against HDAC6. We treated MV4–11 and MOLM–13 cells with 0.1–0.5 μM TH170 for 24 h. We noted that 100 nM TH170 caused a clear reduction of HDAC6 (Fig. 1c).

To cover additional blood cancer entities, we incubated FLT3 wild-type RS4–11 cells (from a 32-year-old female with acute B cell precursor leukemia, B-ALL) and Ramos cells (from a 3-year-old boy with aggressive Burkitt's lymphoma) with 0.1–5 μM TH170 for 24 h. We noted that 100 nM TH170 decreased HDAC6 in such cells as well. This was linked to an accumulation of acetylated tubulin without an increase in acetylated histone H3 (Fig. 1d).

We assessed how higher concentrations of TH170 affected HDAC6 in the four leukemia cell systems. Although 2 μM TH170 reduced HDAC6 effectively in these cells, 5 μM TH170 were ineffective in MV4–11, RS4–11, and Ramos cells, and 10 μM TH170 did not affect HDAC6 in MOLM–13 cells (Fig. 1e). This ineffectiveness of PROTACs at increasing concentrations is known as hook-effect titrating away the E3 ubiquitin ligase [31]. Increasing the concentration of TH170 to 20 μM though reduced HDAC6 significantly. Unlike the attenuation of HDAC6 by lower concentrations of TH170, 20 μM TH170 caused an accumulation of HDAC6 bands that were running faster in the SDS-PAGE (Fig. 1e). This is reminiscent of the cleavage of HDAC6 in leukemia cells that are treated with pro-apoptotic doses of pan-HDACi [9]. This prompted us to analyze the acetylation levels of tubulin and histone H3 in cells treated with 20 μM TH170. Both proteins accumulated in hyperacetylated forms in all four cell types (Fig. 1e).

To assess if the reduction of full-length HDAC6 in leukemia cells that are treated with 20 μM TH170 is linked to apoptosis, we used flow cytometry. We determined the numbers of FLT3 mutant MV4–11 and FLT3 wild-type RS4–11 cells in early and late apoptosis. We could confirm that such doses of TH170 induced apoptosis significantly in both cell systems (Fig. 1f).

These data show that TH170 depletes HDAC6 in various human leukemia cell types.

3.2. Validation of HDAC6 degradation by TH170 through cereblon and proteasomal degradation

Next, we aimed to verify the specificity of TH170 and the anticipated proteasomal degradation of HDAC6 by a cereblon-dependent mechanism. We synthesized TH170E [25]. This analogue of TH170 lacks the hydroxamic acid moiety which binds to the catalytic center of HDACs (Fig. 2a).

We incubated the four leukemia cell lines with the HDAC6 PROTAC TH170, the inactive PROTAC TH170E, and the benzamide entinostat (MS-275). We used this HDACi as positive control for an inhibition of class I HDACs. MS-275 selectively inhibits HDAC1, HDAC2, and HDAC3 and consequently causes an accumulation of hyperacetylated histones in cells [30]. A lack of hyperacetylation of histones in TH170-treated cells in the same experimental settings, i.e., in cells that are susceptible to inhibitors of class I HDACs, can illustrate that this agent does not have an

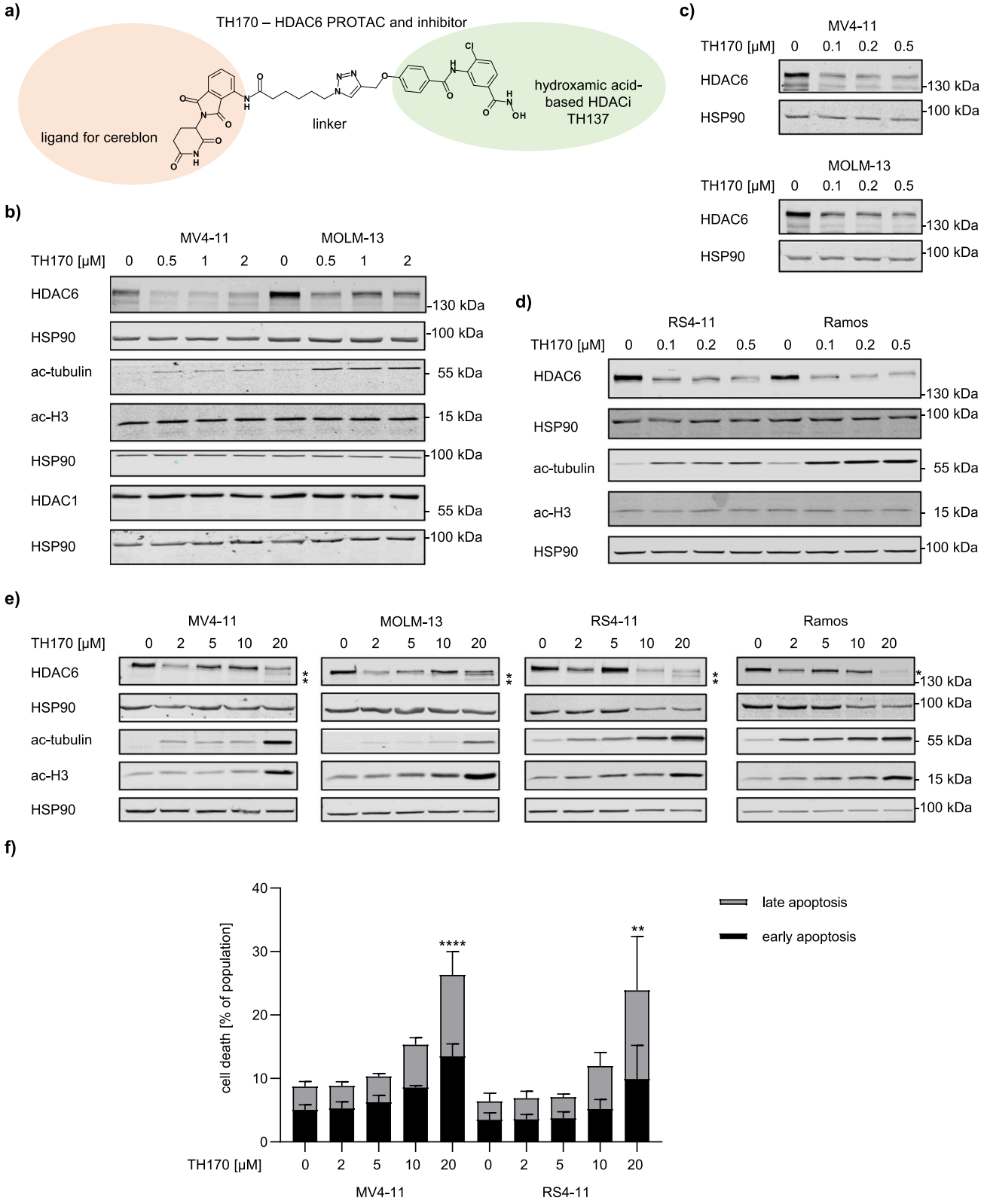

Fig. 1. TH170 depletes HDAC6 in leukemia cells. (a) Shown are the chemical structure of TH170 and its functional domains. (b) Immunoblot analyses were used to detect the concentration-dependent effects of 0.5–2 μM TH170 on MV4–11 and MOLM–13 cells after 24 h. Immunoblot data show HDAC6, acetylated tubulin (ac-tubulin), acetylated histone 3 (ac-H3), and HDAC1; HSP90 detections represent the loading control to ensure equal sample loading. (c) MV4–11 and MOLM–13 cells were incubated for 24 h with 0.1–5 μM TH170. Immunoblot revealed the levels of HDAC6 and the loading control HSP90. (d) RS4–11 and Ramos cells were incubated with 0.1–0.5 μM TH170 for 24 h. (e) The four indicated cell lines were treated with up to 20 μM TH170 and analyzed by immunoblot as indicated; *, HDAC6 fragments. All immunoblots are representative of at least two independent experiments. (f) Annexin/PI staining results for MV4–11 and RS4–11 cells that were treated with the indicated doses of TH170 for 24 h; $n = 3$.

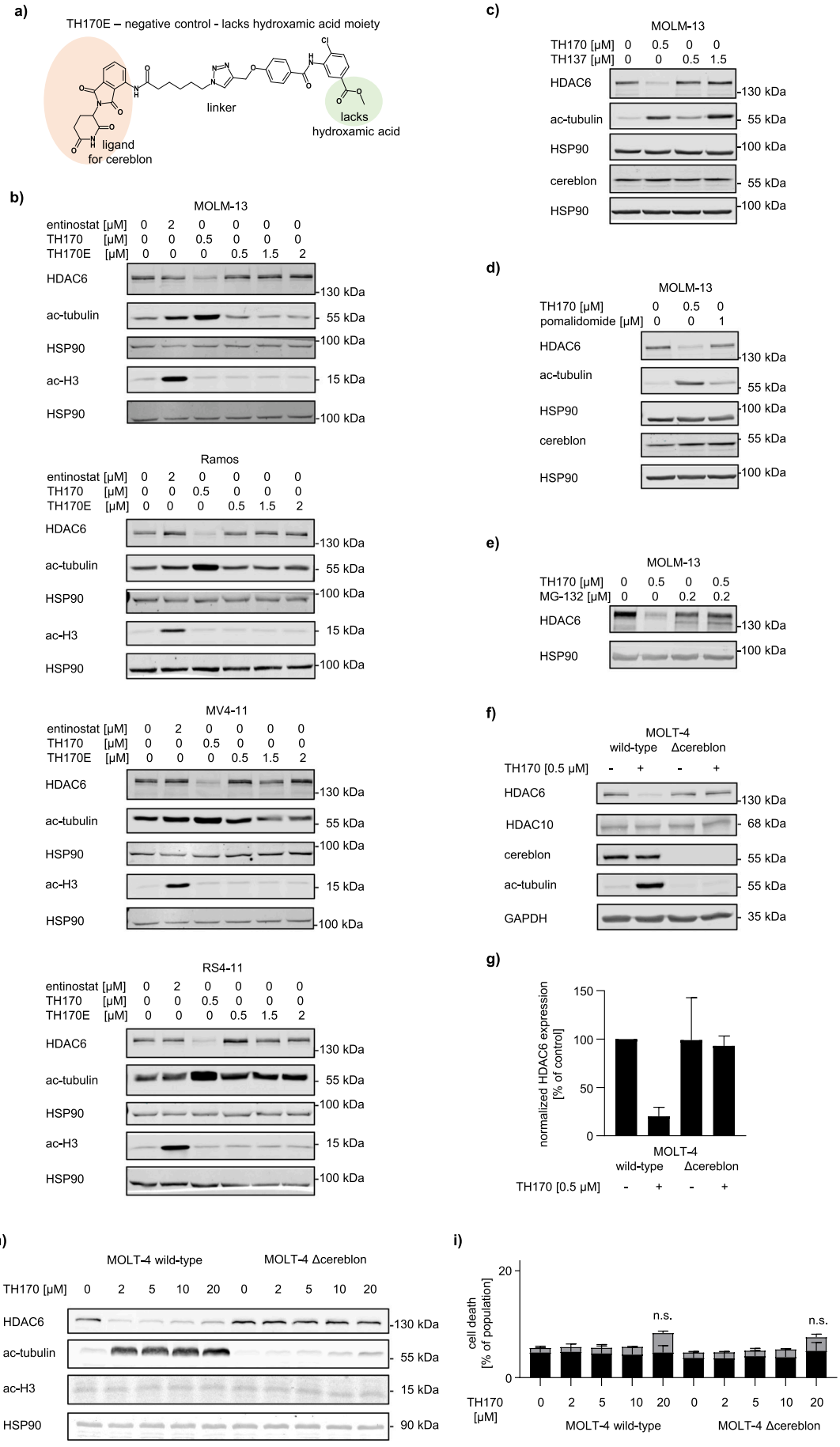

(caption on next page)

Fig. 2. Cereblon-dependent proteasomal degradation of HDAC6. (a) Shown is the chemical structure of TH170E which lacks a hydroxamic acid moiety. (b) MOLM–13, Ramos, MV4–11, and RS4–11 cells were exposed for 24 h to 0.5 μM TH170, 0.5–2 μM TH170E, and 2 μM entinostat. Immunoblot analyses were carried out for acetylated (ac-) tubulin and histone H3; HSP90 represents a control for equal sample loading. (c) MOLM–13 cells were exposed for 24 h to 0.5 μM TH170 and 0.5–1.5 μM TH137. Immunoblot analyses were carried out as mentioned in (b). (d) MOLM–13 cells were treated with TH170 ± pomalidomide for 24 h and analyzed by immunoblot as indicated. (e) Same as in (d), but with 200 nM MG-132. (f) MOLT–4 cells with and without cereblon were plated with 0.5 μM TH170 for 24 h and analyzed by immunoblot as stated. Detection of cereblon verifies the elimination of cereblon. All immunoblots are representative of at least two independent experiments. (g) Quantification of HDAC6 protein levels normalized to the loading control, as measured in 3 independent experiments (one example is shown in 2f). (h) Immunoblot analyses detected the effect of 2–20 μM TH170 on MOLT–4 wildtype and Δcereblon cells after 24 h on HDAC6, acetylated (ac-) tubulin, and acetylated histone H3; HSP90 as loading control; $n = 2$. (i) Flow cytometry results from annexin/PI staining of MOLT–4 wildtype and Δcereblon cells that were treated with the indicated doses of TH170 for 24 h; n = 3.

unspecific effect on class I HDACs. As expected, entinostat increased histone H3 hyperacetylation in all leukemia cell lines (Fig. 2b). The application of 0.5 μM TH170 decreased HDAC6 and caused an accumulation of hyperacetylated tubulin without altering the levels of acetylated histone H3 in these cells. Concentrations of 0.5–2 μM TH170E did not alter the levels of HDAC6 and these acetylation events (Fig. 2b).

To verify that the loss of HDAC6 by TH170 is mediated by the cereblon-recruiting moiety and not by the hydroxamic acid moiety of the inhibitor part, we incubated MOLM–13 cells with the HDAC6 inhibitor TH137. This substance corresponds to TH170 but lacks the cereblon-recruiting ligand. TH137 did not modulate the expression of HDAC6. Concerning the accumulation of acetylated tubulin, we noted that a concentration of 0.5 μM TH137 was less effective than 0.5 μM TH170 (Fig. 2c).

A common assay to verify the specificity of PROTACs for their targets is a competition experiment with the cognate inhibitor molecule [31]. As both TH170 and TH137 can bind and inhibit the catalytic activity of HDAC6, we tested whether the HDAC6 inhibitor TH137 can outcompete the effect of TH170 on HDAC6 in MOLM–13 cells. We could verify the anticipated binding of TH170 to HDAC6 by such a competition experiment using 0.5 μM TH170 and 1.5 μM of the inhibitor TH137. The levels of cereblon were not affected by both agents (Fig. 2c).

To corroborate the cereblon-degradation of HDAC6 by TH170, we used the cereblon ligand pomalidomide. Pomalidomide did not affect the levels of HDAC6 (Fig. 2d), suggesting that pomalidomide does not cause a non-specific reduction of HDAC6. The addition of pomalidomide can saturate cereblon and this can suppress the recruitment of cereblon to cognate PROTACs. Addition of 1 μM pomalidomide attenuated the depletion of HDAC6 by TH170 in MOLM–13 cells partially (**Fig. S1**).

To scrutinize the accelerated proteasomal degradation of HDAC6 in the presence of TH170, we applied TH170 with the proteasome inhibitor MG-132 to MOLM–13 cells. Although this agent affected the stability of HDAC6 by increased cleavage, it blunted the reduction of HDAC6 by TH170 (Fig. 2e).

We could corroborate the loss of HDAC6 by TH170 through cereblon with CRISPR-Cas9 genetically modified MOLT–4 cells that lack cereblon. Incubation of MOLT–4 cells, which are from a 19-year-old man with relapsed T-ALL, with 0.5 μM TH170 reduced HDAC6 and increased tubulin hyperacetylation without notable effects on cereblon itself. In MOLT–4 cells lacking cereblon, TH170 did not affect HDAC6 or the levels of acetylated tubulin (Fig. 2f,g). HDAC6 and HDAC10 are class IIB HDACs. Analyzing HDAC10 by immunoblot, we found that it was not affected by TH170 (Fig. 2f). These data correspond to results that were collected with TH170-treated neuroblastoma cells [25].

We used immunoblotting to assess the FLT3 status of MOLT–4 cells. This approach showed that such cells had low to undetectable levels of FLT3 (**Fig. S2**). We then assessed how up to 20 μM TH170 affected MOLT–4 wild-type and cereblon null cells. Like in the other tested leukemia cells, TH170 reduced HDAC6 with a hook effect but clear accumulation of acetylated tubulin-α over 2–20 μM doses. Unlike in other tested leukemia cells, even 20 μM TH170 did not induce histone H3 hyperacetylation and HDAC6 fragmentation (Fig. 2h).

Coherent with the above-shown association of these processes with apoptosis in MV4–11 and RS4–11 cells (Fig. 1f), 20 μM TH170 did not induce apoptosis of MOLT–4 cells (Fig. 2i).

Data shown in Fig. 2h additionally illustrate that 10 μM TH170 induces a weak accumulation of acetylated tubulin in MOLT–4 cells without cereblon. This finding reveals that the effects of TH170 on HDAC6 and acetylated tubulin rely mainly on proteasomal degradation of HDAC6 and weakly on the TH137 moiety, i.e., the HDAC6 inhibitor moiety.

These results verify that TH170 depletes HDAC6 by a cereblon-dependent proteasomal degradation mechanism and that this is the main effect of TH170 on HDAC6.

3.3. TH170 does not deplete tumor-promoting proteins and does not damage DNA

Above, we note that there are contradicting results on whether HDAC6 affects tumor growth. We investigated if TH170 altered the levels of oncological relevant proteins. Two of our cell models, MV4–11 and MOLM–13 cells, carry the hyperactive tyrosine kinase FLT3-ITD homo- or heterozygous. We treated them with 0.5–2 μM TH170, TH170E, or 2–5 μM entinostat for 24 h. While TH170 and TH170E did not modulate FLT3-ITD, 5 μM entinostat reduced it. We made similar observations for the transcription factor MYC (Fig. 3a) which is frequently involved in tumorigenesis [32]. We next evaluated the expression of the tumor-suppressive transcription factor p53 and the autophagy regulator beclin-1 [33]. None of the compounds affected them (Fig. 3a).

Since the ubiquitin-specific protease USP10 was reported to control the levels of FLT3-ITD [34], we determined if TH170, TH170E, or entinostat affected USP10. None of these agents altered USP10 expression in MV4–11 and MOLM–13 cells (**Fig. S3**).

For further investigations, we extended the incubation times with TH170 and entinostat to 72 h. In MOLM–13 (FLT3-ITD/FLT3), MV4–11 (FLT3-ITD/FLT3-ITD), Ramos, and RS4–11 (FLT3) cells, TH170 reduced HDAC6 and augmented tubulin acetylation for up to 72 h. This was not associated with alterations in the levels of wild-type FLT3 and FLT3-ITD; Ramos cells have low levels of FLT3. Entinostat reduced HDAC6 in the cell lines, but this was not consistently associated with tubulin hyperacetylation (Fig. 3b).

As tumorigenesis is often linked to DNA stress, we analyzed if TH170 had an impact on the DNA repair protein RAD51 [35] and the DNA replication stress/DNA damage and apoptosis marker histone H2AX phosphorylated at S139 (γH2AX) [36]. Entinostat reduced RAD51 and caused an accumulation of γH2AX. TH170 did not modulate these proteins (Fig. 3c).

These data demonstrate that TH170 does not affect a set of tumor-relevant proteins and does not induce biochemical markers of DNA lesions.

3.4. Lack of cellular activity of TH170 despite high biochemical activity

Having identified that TH170 eliminated HDAC6 in leukemic cells, we analyzed the biological impact of TH170. We incubated the four leukemia cell types with 0.5–2 μM TH170 or 2 μM entinostat for 72 h and evaluated biochemical markers of apoptosis by immunoblot. Entinostat induced an accumulation of activated caspase-3, the ultimate executioner of apoptosis, and the accumulation of cleaved PARP1, a

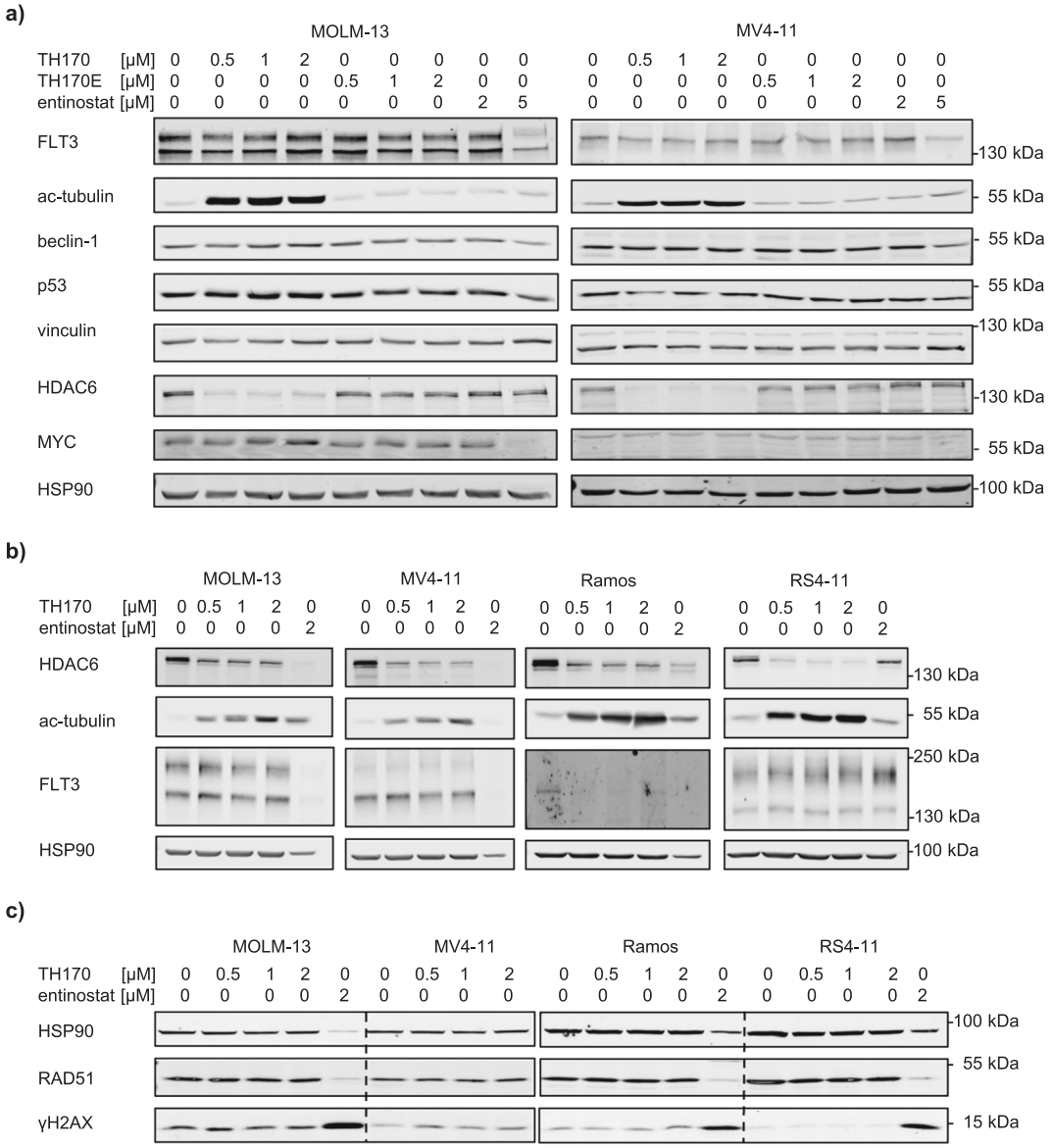

Fig. 3. Class I HDACs control survival proteins. (a) MOLM–13 and MV4–11 cells were treated as indicated for 24 h and analyzed by immunoblot. (b) The four leukemia cell types were incubated with TH170 or the class I HDACi entinostat for 72 h. Lysates of these cells were subjected to immunoblot analyses. (c) Same as in b) with analysis of DNA replication stress/DNA damage proteins. All immunoblots are representative of at least two independent experiments.

prototypical substrate of caspase-3 (Fig. 4a).

We then determined how 0.5 μM TH170 affected the proliferation of these cell types. After four to five days, three of the untreated and TH170-treated leukemia cell types grew equally well. There was a slight reduction in the growth of RS4–11 cells, but this effect was not significant and lasting (Fig. 4b and data not shown). This was not due to lost activity of TH170. In lysates of all four cell types, we noted reduced levels of HDAC6 and accumulation of acetylated tubulin after a four-day treatment with TH170 (Fig. 4c).

We asked how these data could be reconciled with large datasets in the DepMap database that was created by the Broad Institute. Data therein show that a CRISPR-Cas9-mediated elimination of HDAC6 in 91 lymphoid and 37 myeloid human leukemia cell lines has a very mild to no impact on their proliferation. Normal myeloid cells were also unaffected by the elimination of HDAC6 (Fig. 4d).

These results of an unaltered cell proliferation in the presence of TH170 are consistent with the data that we collected with immunoblotting.

3.5. TH170 inhibits HDAC6 in human lung epithelial cells at nontoxic concentrations

The data above disfavor that a pharmacological elimination of HDAC6 is a valid anti-cancer option. Since HDAC6 modulates the replication of IAV both dependently and independently of its catalytic activity [19], we asked if TH170 might be effective against IAV. The respiratory system is the first contact site for IAV. We assessed HDAC6 expression in The Human Protein Atlas. This database, which contains single-cell sequencing analyses, shows that the *HDAC6* mRNA is expressed in bronchus and lung (**Fig. S4**). This indicates that HDAC6 is a potential drug target in the primary infection site of IAV.

We examined the effects of TH170 and its controls on HDAC6 expression as well as on the morphology and the vitality of human alveolar basal epithelial A549 cells (from the adenocarcinoma of a 58-year-old male). We used immunoblotting, light microscopy, and MTT assay which measures metabolic activity as readout for cellular fitness. We treated these cells for 36 h with 0.25–4 μM TH170 and up to 2 μM of the HDAC6 inhibitor TH137. Although A549 cells are less sensitive to

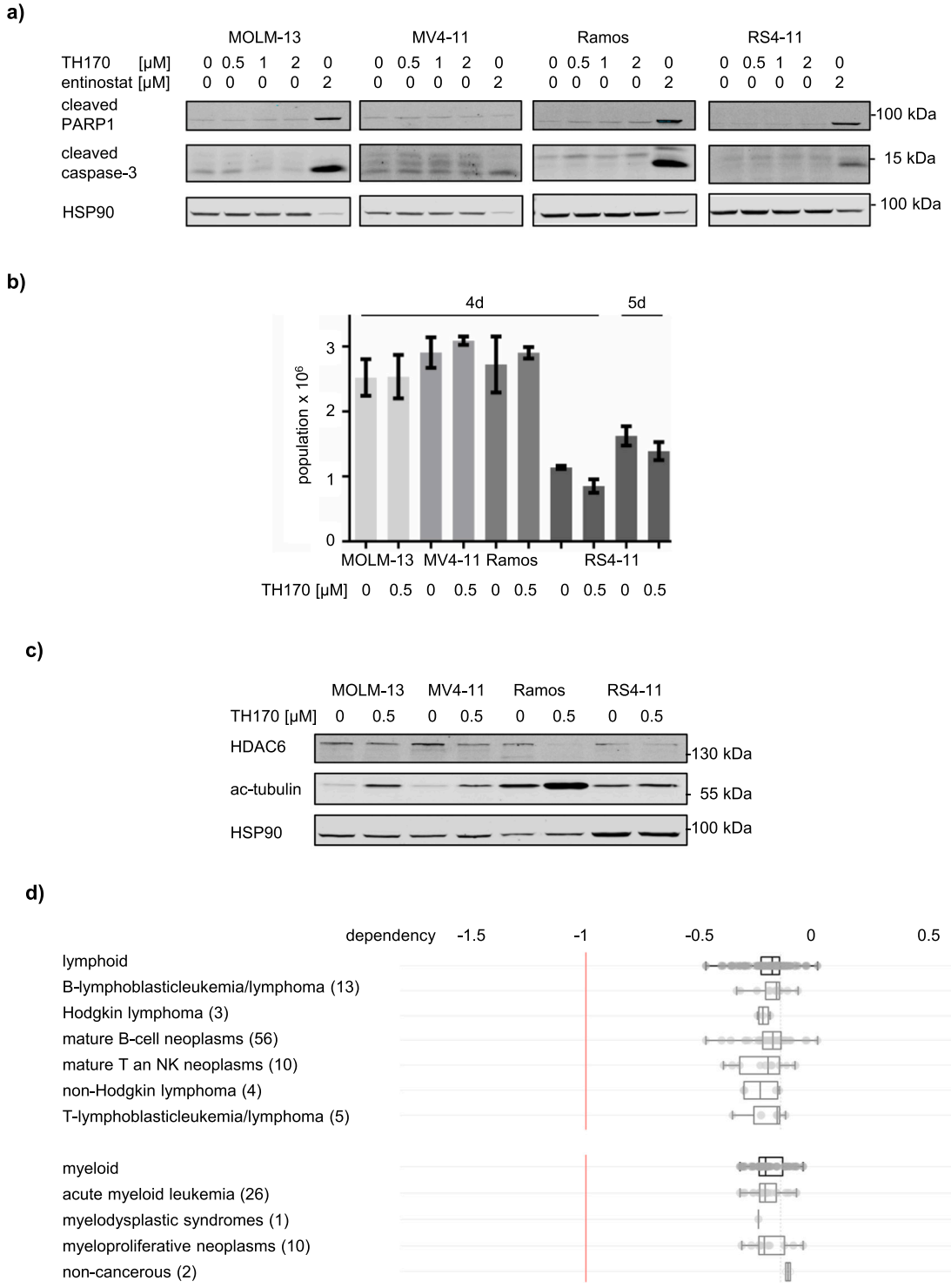

Fig. 4. Targeted proteolysis of HDAC6 does not kill leukemia cells. (a) The four leukemia cell types were incubated with HDACi as stated for 72 h. Lysates of these cells were analyzed for the indicated apoptosis proteins by immunoblot. (b) The proliferation of the cells in the presence of 0.5 μM TH170 was determined by counting after 4–5 d. (c) Lysates of these cells were collected after 4 d and subjected to immunoblot assessing the HDAC6-acetylated tubulin axis. (d) The DepMap database shows that CRISPR-Cas9-mediated deletions of HDAC6 in transformed lymphoid and myeloid cells and non-cancerous myeloid cells have no adverse effects on their proliferation. Negative values indicate that the cells depend on the deleted gene, respectively the encoded protein. The values below −1 indicate that the cells require the analyzed gene. All immunoblots are representative of at least two independent experiments.

HDAC6 depletion by TH170, they show a clear TH170 dose-dependent elimination of HDAC6 and a concurrent accumulation of acetylated tubulin. The application of up to 4 μM TH170 evoked no hook-effect in A549 cells. TH137 was significantly less active in such cells, illustrating a higher potency of the PROTAC TH170 compared to the HDAC6 inhibitor TH137 in this model (Fig. 5a). Therefore, we used 5 μM of TH170, its negative control compound TH170E, and TH137 (the HDACi building block of TH170) in subsequent experiments. This concentration of TH170 decreased HDAC6 in A549 cells (**Fig. S5**).

To assess if such drug concentrations are toxic to A549 cells, we

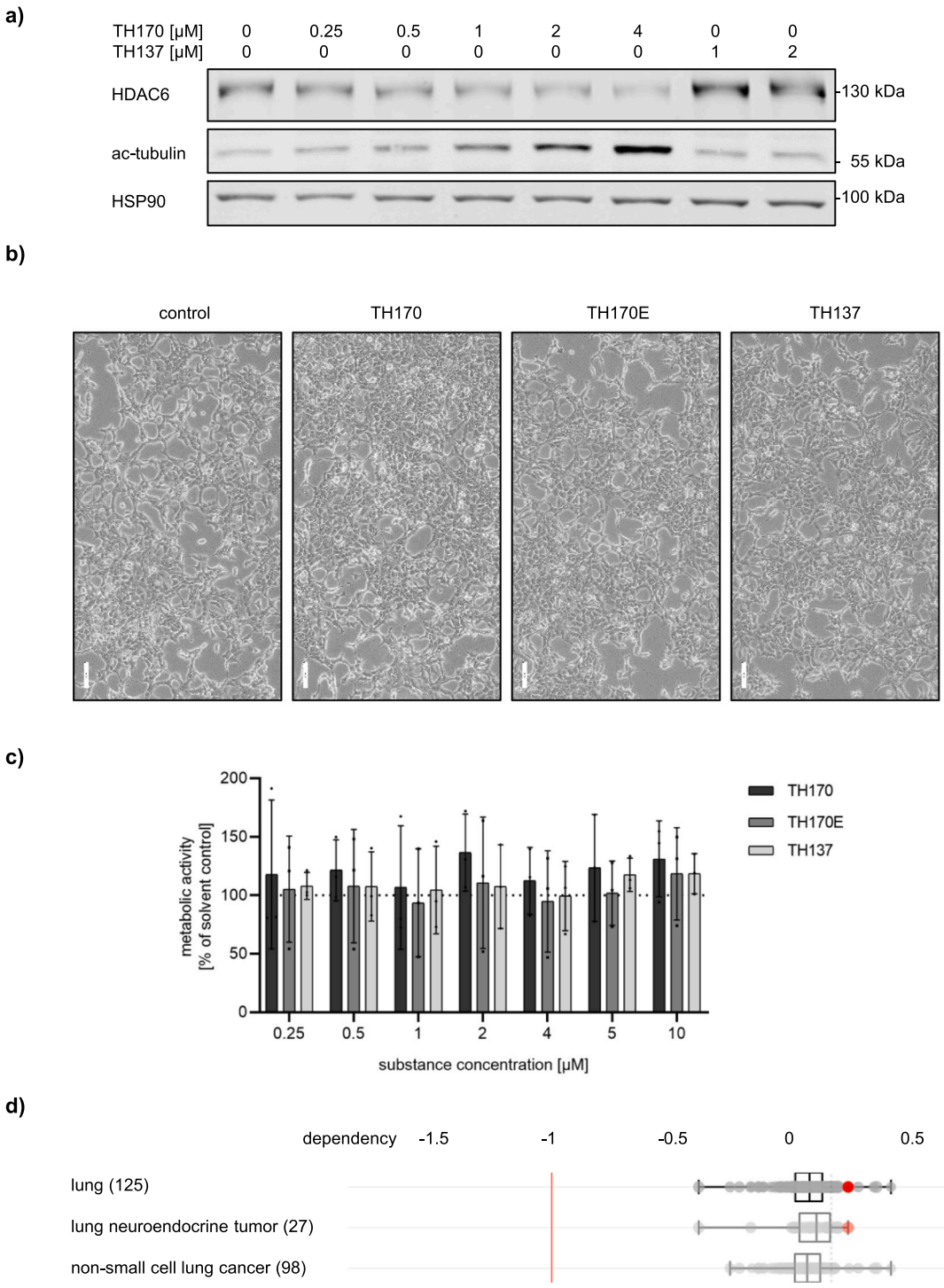

Fig. 5. TH170 depletes HDAC6 without causing cytotoxicity to lung-derived cancer cells. (a) Concentration-dependent effects of 0.25–4 µM TH170 and 1-2 µM TH137 on A549 cells after 36 h. Immunoblot analyses were used to detect HDAC6 and acetylated tubulin. HSP90 represents the loading control to ensure equal sample concentrations. (b) A549 cells were treated with 5 µM TH170, TH170E, and TH137, or DMSO as solvent control. The impact of the compounds on cell morphology was visualized by an AxioVert.A1 microscope (10-fold magnification) and monitored by an Axiocam 208 color camera after 36 h. Representative images are shown. Scale bars represent 50 µM. (c) A549 cells were treated with the solvent DMSO as control, TH170, TH170E, or TH137 in the indicated concentrations for 36 h. The metabolic activities of cellular samples were determined by colorimetric assays using the MTT assay and are shown as relative values in comparison to DMSO-treated control cell samples, which were arbitrarily set to 100 %. Data represent mean ± SD of three independent experiments including three biological samples. (d) DepMap analysis shows that 125 lung cancer cell lines grow independently of HDAC6; red dots indicate cell lines with mutant HDAC6 loci. (For interpretation of the references to color in this figure legend, the reader is referred to the web version of this article.)

analyzed their morphology. We found no disturbance of cell layers and no visible cytotoxic effects on cell morphology after treatment with these agents after 36 h (Fig. 5b). Using the MTT-test, we confirmed that none of these agents had a negative impact on these cells using substance concentration between 0.25 and 10 μM (Fig. 5c). Coherent herewith, the DepMap database shows that the genetic elimination of HDAC6 by CRISPR-Cas9 does not compromise the growth of 125 lung cancer cells (Fig. 5d).

Hence, TH170 attenuates HDAC6 in lung cancer cells which do not seem to rely on HDAC6.

3.6. Inhibition of HDAC6 attenuates the replication of influenza A virus

Next, we studied how the presence of HDAC6 affected the propagation of IAV in multicycle replication experiments 24 h post infection (p.i.). A549 cells were treated with TH170, TH170E, or TH137 for 12 h, infected for 1 h with 1 MOI IAV, and incubated with these agents until 24 h p.i. IAV progeny production of the PR8 strain was significantly reduced at 24 h p.i. in presence of TH170 compared to the solvent control (ctrl) (Fig. 6a). The controls TH170E (inactive PROTAC) as well as the inhibitor TH137 had no effect on viral replication. In comparison, the progeny production of the Jena/5258 strain was slightly reduced after treatment with the PROTAC TH170 and the inhibitor TH137 (Fig. 6c). Immunoblot analyses showed a decrease in HDAC6 and an

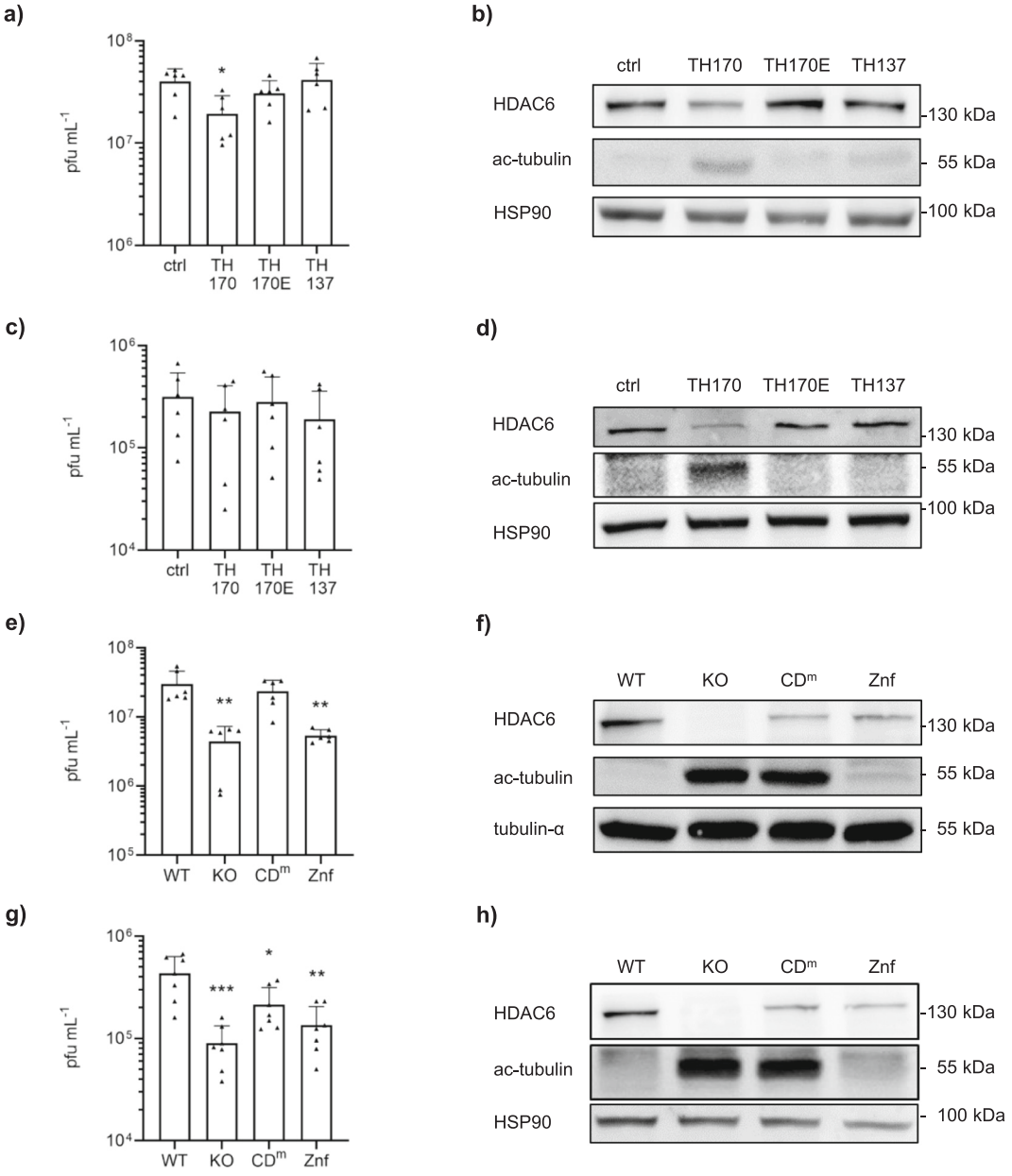

Fig. 6. TH170 attenuates IAV replication of different IAV strains. (a - d) Cells were treated with 5 μM TH170, TH170E, TH137, or DMSO as solvent control (ctrl) for 12 h. Thereafter, cells were infected with 1.0 MOI of (a, b) PR8 or (c, d) Jena/5258 for 1 h. After medium change, cells were further incubated in the absence or presence of the compounds for up to 24 h p.i. (e - h) A549 WT, A549-HDAC6^{KO}, A549-HDAC6^{CDm}, and A549-HDAC6^{Znf} cells were infected with 1.0 MOI of (e, f) PR8 or (g, h) Jena/5258 for 1 h. (a, c, e, g) Virus concentrations were determined in supernatants by standard plaque assays 24 h p.i. Results of virus titrations are means (+SD) of three independent experiments, including two biological replicates. Statistical significance was analyzed by unpaired two-tailed *t*-tests against the control or the WT (*, $p < 0.0115$; **, $p < 0.0021$; ***, $p = 0.0008$). (b, d, f, h) Immunoblots were used to analyze levels of HDAC6, acetylated tubulin, and the loading controls HSP90 or tubulin-α. All immunoblots are representative of at least three independent experiments.

increase in acetylated tubulin in TH170-treated samples when using both viruses (Fig. 6**b** and **d**).

Using a genetic approach, we analyzed whether a complete loss of HDAC6 affected IAV replication. For that we used A549 wild-type (WT) cells, A549-HDAC6^{KO} cells that lack HDAC6, A549 cells with a mutation in the second catalytic domain of HDAC6 (A549-HDAC6^{CDm}), and A549 cells with a mutated zinc finger domain (A549-HDAC6^{Znf}) [18]. In accordance with the TH170-mediated elimination of HDAC6, A549-HDAC6^{KO} as well as A549-HDAC6^{Znf} cells revealed significantly decreased virus yields of both IAV strains at 24 h p.i. compared to A549 WT cells (Fig. 6**e** and **g**). Loss of the second catalytic domain of HDAC6 had no influence on viral replication of the PR8 strain but a weak decreasing effect on the replication of the Jena/5258 strain. We confirmed the absence of HDAC6 in A549-HDAC6^{KO} cells by immunoblot analyses. In addition, A549-HDAC6^{CDm} and A549-HDAC6^{Znf} cells showed a reduced HDAC6 protein expression. A549-HDAC6^{KO} and A549-HDAC6^{CDm} cells revealed a strong expression of acetylated tubulin, which was only very weakly detectable in A549-HDAC6^{Znf} cells (Fig. 6**f** and **h**).

These data indicate that pharmacological and genetic elimination of HDAC6 interferes with the propagation of IAV in lung-derived cells.

4. Discussion

Our data show that the PROTAC TH170 can inhibit and eliminate HDAC6 in leukemic cells. This effect occurs with a hook-effect, i.e., the effect is induced concentration-dependently in a certain dose range and lost with higher drug concentrations [31]. This might be explained by high doses of TH170 blocking access of the ubiquitination machinery to HDAC6. Alternatively, high levels of TH170 might occupy free cereblon that can induce the poly-ubiquitination of HDAC6. In the case of TH170, we noted a decrease of HDAC6 with doses beyond the ones inducing the hook-effect. Unlike the reduction of HDAC6 by lower concentrations of TH170, these higher doses of TH170 led to the appearance of HDAC6 fragments with lower molecular weights. This is linked to apoptotic cell death, which can be explained by a non-selective reduction of class I HDACs. This is evidenced by the accumulation of acetylated forms of histone H3 in response to high doses of TH170. It must be considered that histone H3 is not a substrate of HDAC6 and, accordingly, high concentrations of TH170 are not suitable to assess specific functions of HDAC6. Coherent with our previously published works [9,10,37], we found that an inhibition of class I HDACs but not of HDAC6 decreased MYC and FLT3-ITD in AML cells.

The data that we collected with cereblon null cells and immunoblotting for the HDAC6-acetyl-tubulin-axis disclose that TH170 is a bona fide targeted degrader of HDAC6 without a significantly detectable HDAC6 inhibitor activity at concentrations up to at least 10 μM. We currently cannot exclude that an inhibition of HDAC6 without induction of its degradation is more useful to treat diseases. Human HDAC6 has 1215 amino acids and several functionally important domains. These include an N-terminal domain anchoring HDAC6 to tubulin, two catalytically active domains with individual substrates, and a C-terminal domain that is important for the clearance of damaged proteins [3]. Hence, blocked HDAC6 may exert structural, biologically important functions. Future work is necessary to elaborate on the unexplored possibility that an inhibition of the catalytic center(s) of the HDAC6 molecule causes an impact on the fate of certain cell types that an elimination of HDAC6 cannot produce. For example, this may be the case in aggressive B-cell lymphoma cells [38].

There are multiple known functions of HDAC6 beyond its catalytic activity. In addition to the well-established functions of the ubiquitin-binding domain of HDAC6 [3,39], the primate-specific SE14 repeat domain of HDAC6 has been identified to mediate biologically important functions [40]. Further studies are also necessary to delineate how HDAC6 inhibition and elimination controls HDAC6's impact on tumor immunology [41]. Thus, the lack of anti-proliferative effects of HDAC6 inhibition and elimination does not preclude beneficial effects of this strategy per se. Immune modulatory functions in autoimmunity [9] as well as modulatory effects on the tumor environment [41] may be possible with drug doses that specifically inhibit HDAC6.

Adherent A549 cells are more resistant to drug treatment than AML cells in suspension. Therefore, higher but still not toxic concentrations of TH170 are required to inhibit HDAC6 and accumulate acetylated tubulin in cells. The ubiquitin binding activity of HDAC6 is involved in the uncoating process of IAV [17–19]. We analyzed the impact of TH170 on the production of IAV by A549 WT cells, and in A549-HDAC6^{KO}, A549-HDAC6^{CDm}, and A549-HDAC6^{Znf} cells. Consistent with previous studies, a significant decrease of viral replication was shown in A549-HDAC6^{KO} and A549-HDAC6^{Znf} cells but not in A549-HDAC6^{CDm} cells [17–19]. This suggests that the second catalytic domain of HDAC6 is crucial for its deacetylation activity but not involved in IAV replication. However, the zinc finger domain has no deacetylating activity but is essential for IAV replication due to its ubiquitin binding capacity. Both IAV strains, the laboratory strain PR8 as well as the clinical isolate Jena/5258, revealed similar reactions in the context of the presence or absence of HDAC6 activity. However, the Jena/5258 strain was less effective at replicating in A549 cells, which might account for the less pronounced virus-inhibiting effect of TH170. One reason for this might be the lack of adaptation of the Jena/5258 strain to the established cell line A549 in vitro. However, consistent results regarding the importance of the zinc finger domain of HDAC6 for the replication of PR/8 and Jena/5258 were obtained using our genetic approach. Therein, the structure of HDAC6 itself is more important than its catalytic activity in the context of IAV replication. Hence, a deeper and more effective pharmacological elimination of HDAC6 than with TH170 may trigger better anti-viral effects. The design of such compounds can involve the recruitment of other E3 ubiquitin ligases, other linkers and zinc-binding domains, but also alternative approaches including hydrophobic tagging molecules and further proximity-inducing drugs [28,42,43].

The low toxicity of HDAC6 inhibitors and PROTACs for HDAC6 corresponds to in vivo data. Even a full body constitutive elimination of both *Hdac6* alleles in mice does not compromise their growth and development [15]. On the one hand, this dispensable role of HDAC6 may blunt pharmacological approaches that target HDAC6 in most tumor cells. On the other hand, the toxicological safety of such approaches for normal cells may pave the way for novel, efficient anti-viral strategies with heterobifunctional degraders against HDAC6. Thus, screening anti-IAV effects of future HDAC6 degraders may be an option to optimize such agents for prospective in vivo approaches.

CRediT authorship contribution statement

Johannes Jungwirth: Writing – review & editing, Visualization, Validation, Methodology, Investigation, Formal analysis, Data curation. **Andreas O. Mieland:** Validation, Investigation, Formal analysis, Data curation. **Andrea Piée-Staffa:** Validation, Methodology, Investigation, Formal analysis. **Tino Heimburg:** Resources. **Walburgis Brenner:** Resources, Conceptualization. **Christina Ehrhardt:** Writing – review & editing, Resources. **Wolfgang Sippl:** Writing – review & editing, Resources, Conceptualization. **Andreas Henke:** Writing – original draft, Resources, Project administration, Funding acquisition, Data curation, Conceptualization. **Oliver H. Krämer:** Writing – original draft, Supervision, Project administration, Funding acquisition, Data curation, Conceptualization.

Funding

This work was made possible with funding from the German Research Foundation/Deutsche Forschungsgemeinschaft (DFG) grant HE2910/16–1 and KR2291/17–1, DFG-project number 502534123 to A. H. and O.H.K. Work done in the group of O.H.K. is additionally funded by the DFG grant KR2291/12–1, DFG-project number 445785155;

KR2291/9–1, DFG-project number 427404172; KR2291/14–1, DFG-project number 469954457; KR2291/15–1, DFG-project number 495271833; KR2291/16–1, DFG-project number 496927074; DFG-project number 393547839 - SFB 1361, sub-project 11; the Walter Schulz Stiftung; the Brigitte und Dr. Konstanze Wegener-Stiftung (projects 65/110); the Deutsche José Carreras Leukämie-Stiftung, and the Hector Stiftung Weinheim. Work done in the group of W.S. was funded by the DFG grant SI868/22–1, DFG-project number 469954457, DFG grant SI868/27–1, DFG-project number 503267011.

Declaration of competing interest

OHK declares the patents "The use of molecular markers for the preclinical and clinical profiling of inhibitors of enzymes having histone deacetylase activity, WO/2004/027418", "Novel HDAC6 inhibitors and their uses, WO2016020369A1", and "Synthesis, pharmacology and use of new and selective FMS-like tyrosine kinase 3 (FLT3) inhibitors, WO2019/034538", and advisory consultant activity for BASF, Ludwigshafen, Germany. The substances that are covered in these patents are not those that are shown herein and BASF has not produced these compounds for us. Thus, there are no direct competing interests.

Acknowledgements

We thank Prof. Dr. Patrick Matthias, Basel, and Dr. Georg E. Winter, Vienna, for cell lines that supported the success of this project. We thank Dr. Matthias Schmidt for support in the analytical characterization and purification of the PROTAC.

Appendix A. Supplementary data

Supplementary data to this article can be found online at https://doi.org/10.1016/j.lfs.2025.123401.

Data availability

Data will be made available on request.

References

[1] G. Li, Y. Tian, W.G. Zhu, The roles of histone deacetylases and their inhibitors in Cancer therapy, Front. Cell Dev. Biol. 8 (2020) 576946.
[2] A.M. Mustafa, O.H. Krämer, Pharmacological modulation of the crosstalk between aberrant Janus kinase signaling and epigenetic modifiers of the histone deacetylase family to treat Cancer, Pharmacol. Rev. 75 (1) (2023) 35–61.
[3] O.H. Krämer, S. Mahboobi, A. Sellmer, Drugging the HDAC6-HSP90 interplay in malignant cells, Trends Pharmacol. Sci. 35 (10) (2014) 501–509.
[4] P. Bali, P. George, P. Cohen, J. Tao, F. Guo, C. Sigua, A. Vishvanath, A. Scuto, S. Annavarapu, W. Fiskus, L. Moscinski, P. Atadja, K. Bhalla, Superior activity of the combination of histone deacetylase inhibitor LAQ824 and the FLT-3 kinase inhibitor PKC412 against human acute myelogenous leukemia cells with mutant FLT-3, Clin. Cancer Res. 10 (15) (2004) 4991–4997.
[5] R. Rao, W. Fiskus, Y. Yang, P. Lee, R. Joshi, P. Fernandez, A. Mandawat, P. Atadja, J.E. Bradner, K. Bhalla, HDAC6 inhibition enhances 17-AAG–mediated abrogation of hsp90 chaperone function in human leukemia cells, Blood 112 (5) (2008) 1886–1893.
[6] M. Leonhardt, A. Sellmer, O.H. Krämer, S. Dove, S. Elz, B. Kraus, M. Beyer, S. Mahboobi, Design and biological evaluation of tetrahydro-beta-carboline derivatives as highly potent histone deacetylase 6 (HDAC6) inhibitors, Eur. J. Med. Chem. 152 (2018) 329–357.
[7] K. Noack, N. Mahendrarajah, D. Hennig, L. Schmidt, F. Grebien, D. Hildebrand, M. Christmann, B. Kaina, A. Sellmer, S. Mahboobi, K. Kubatzky, T. Heinzel, O. H. Krämer, Analysis of the interplay between all-trans retinoic acid and histone deacetylase inhibitors in leukemic cells, Arch. Toxicol. 91 (5) (2017) 2191–2208.
[8] M. Pons, G. Nagel, Y. Zeyn, M. Beyer, T. Laguna, T. Brachetti, A. Sellmer, S. Mahboobi, R. Conradi, F. Butter, O.H. Krämer, Human platelet lysate as validated replacement for animal serum to assess chemosensitivity, ALTEX 36 (2) (2019) 277–288.
[9] A. Sellmer, H. Stangl, M. Beyer, E. Grünstein, M. Leonhardt, H. Pongratz, E. Eichhorn, S. Elz, B. Striegl, Z. Jenei-Lanzl, S. Dove, R.H. Straub, O.H. Krämer, S. Mahboobi, Marbostat-100 defines a new class of potent and selective Antiinflammatory and Antirheumatic histone deacetylase 6 inhibitors, J. Med. Chem. 61 (8) (2018) 3454–3477.
[10] M. Beyer, A. Romanski, A.M. Mustafa, M. Pons, I. Buchler, A. Vogel, A. Pautz, A. Sellmer, G. Schneider, G. Bug, O.H. Krämer, HDAC3 activity is essential for human leukemic cell growth and the expression of beta-catenin, MYC, and WT1, Cancers (Basel) 11 (10) (2019).
[11] Y. Depetter, S. Geurs, R. De Vreese, S. Goethals, E. Vandoorn, A. Laevens, J. Steenbrugge, E. Meyer, P. de Tullio, M. Bracke, M. D'Hooghe, O. De Wever, Selective pharmacological inhibitors of HDAC6 reveal biochemical activity but functional tolerance in cancer models, Int. J. Cancer 145 (3) (2019) 735–747.
[12] J.J. Bandolik, A. Hamacher, C. Schrenk, R. Weishaupt, M.U. Kassack, Class I-histone deacetylase (HDAC) inhibition is superior to pan-HDAC inhibition in modulating cisplatin potency in high grade serous ovarian Cancer cell lines, Int. J. Mol. Sci. 20 (12) (2019).
[13] K. Toutah, N. Nawar, S. Timonen, H. Sorger, Y.S. Raouf, S. Bukhari, J. von Jan, A. Ianevski, J.M. Gawel, O.O. Olaoye, M. Geletu, A. Abdeldayem, J. Israelian, T. B. Radu, A. Sedighi, M.N. Bhatti, M.M. Hassan, P. Manaswiyoungkul, A. E. Shouksmith, H.A. Neubauer, E.D. de Araujo, T. Aittokallio, O.H. Krämer, R. Moriggl, S. Mustjoki, M. Herling, P.T. Gunning, Development of HDAC inhibitors exhibiting therapeutic potential in T-cell prolymphocytic leukemia, J. Med. Chem. 64 (12) (2021) 8486–8509.
[14] L. Sinatra, J. Yang, J. Schliehe-Diecks, N. Dienstbier, M. Vogt, P. Gebing, L. M. Bachmann, M. Sönnichsen, T. Lenz, K. Stuhler, A. Schöler, A. Borkhardt, S. Bhatia, F.K. Hansen, Solid-phase synthesis of Cereblon-recruiting selective histone deacetylase 6 degraders (HDAC6 PROTACs) with Antileukemic activity, J. Med. Chem. 65 (24) (2022) 16860–16878.
[15] Y. Zhang, S. Kwon, T. Yamaguchi, F. Cubizolles, S. Rousseaux, M. Kneissel, C. Cao, N. Li, H.L. Cheng, K. Chua, D. Lombard, A. Mizeracki, G. Matthias, F.W. Alt, S. Khochbin, P. Matthias, Mice lacking histone deacetylase 6 have hyperacetylated tubulin but are viable and develop normally, Mol. Cell. Biol. 28 (5) (2008) 1688–1701.
[16] Y.W. Wang, L. Lan, M. Wang, J.Y. Zhang, Y.H. Gao, L. Shi, L.P. Sun, PROTACS: a technology with a gold rush-like atmosphere, Eur. J. Med. Chem. 247 (2022) 115037.
[17] I. Banerjee, Y. Miyake, S.P. Nobs, C. Schneider, P. Horvath, M. Kopf, P. Matthias, A. Helenius, Y. Yamauchi, Influenza a virus uses the aggresome processing machinery for host cell entry, Science 346 (6208) (2014) 473–477.
[18] A. Artcibasova, L. Wang, S. Anchisi, Y. Yamauchi, M. Schmolke, P. Matthias, J. Stelling, A quantitative model for virus uncoating predicts influenza a infectivity, Cell Rep. 42 (12) (2023) 113558.
[19] E.A. Moreira, Y. Yamauchi, P. Matthias, How influenza virus uses host cell pathways during Uncoating, Cells 10 (7) (2021).
[20] L. Wang, E.A. Moreira, G. Kempf, Y. Miyake, B.I. Oliveira Esteves, A. Fahmi, J. V. Schaefer, B. Dreier, Y. Yamauchi, M.P. Alves, A. Pluckthun, P. Matthias, Disrupting the HDAC6-ubiquitin interaction impairs infection by influenza and Zika virus and cellular stress pathways, Cell Rep. 39 (4) (2022) 110736.
[21] M. Husain, C.Y. Cheung, Histone deacetylase 6 inhibits influenza a virus release by downregulating the trafficking of viral components to the plasma membrane via its substrate, acetylated microtubules, J. Virol. 88 (19) (2014) 11229–11239.
[22] M. Husain, K.S. Harrod, Enhanced acetylation of alpha-tubulin in influenza a virus infected epithelial cells, FEBS Lett. 585 (1) (2011) 128–132.
[23] S.J. Choi, H.C. Lee, J.H. Kim, S.Y. Park, T.H. Kim, W.K. Lee, D.J. Jang, J.E. Yoon, Y. I. Choi, S. Kim, J. Ma, C.J. Kim, T.P. Yao, J.U. Jung, J.Y. Lee, J.S. Lee, HDAC6 regulates cellular viral RNA sensing by deacetylation of RIG-I, EMBO J. 35 (4) (2016) 429–442.
[24] H. Chen, Y. Qian, X. Chen, Z. Ruan, Y. Ye, H. Chen, L.A. Babiuk, Y.S. Jung, J. Dai, HDAC6 restricts influenza a virus by deacetylation of the RNA polymerase PA subunit, J. Virol. 93 (4) (2019).
[25] S. Darwish, T. Heimburg, J. Ridinger, D. Herp, M. Schmidt, C. Romier, M. Jung, I. Oehme, W. Sippl, Synthesis, biochemical, and cellular evaluation of HDAC6 targeting proteolysis targeting chimeras, Methods Mol. Biol. 2589 (2023) 179–193.
[26] N. Seidel, A. Sauerbrei, P. Wutzler, M. Schmidtke, Hemagglutinin 222D/G polymorphism facilitates fast intra-host evolution of pandemic (H1N1) 2009 influenza a viruses, PLoS One 9 (8) (2014) e104233.
[27] A. Nguyen, A.M. Mustafa, A.K. Leydecker, M. Halilovic, J. Murr, F. Butter, O. H. Krämer, The protein phosphatase-2A subunit PR130 is involved in the formation of cytotoxic protein aggregates in pancreatic ductal adenocarcinoma cells, Cell Commun. Signal 22 (1) (2024) 217.
[28] M. Halilovic, M. Abdelsalam, J. Zabkiewicz, M. Lazenby, C. Alvares, M. Schmidt, W. Brenner, S. Najafi, I. Oehme, C. Hieber, Y. Zeyn, M. Bros, W. Sippl, O.H. Krämer, Selective degradation of mutant FMS-like tyrosine kinase-3 requires BIM-dependent depletion of heat shock proteins, Leukemia 38 (12) (2024) 2561–2572.
[29] T. Heimburg, F.R. Kolbinger, P. Zeyen, E. Ghazy, D. Herp, K. Schmidtkunz, J. Melesina, T.B. Shaik, F. Erdmann, M. Schmidt, C. Romier, D. Robaa, O. Witt, I. Oehme, M. Jung, W. Sippl, Structure-based design and biological characterization of selective histone deacetylase 8 (HDAC8) inhibitors with anti-neuroblastoma activity, J. Med. Chem. 60 (24) (2017) 10188–10204.
[30] M. Beyer, N. Kiweler, S. Mahboobi, O.H. Krämer, How to distinguish between the activity of HDAC1-3 and HDAC6 with Western blot, Methods Mol. Biol. 1510 (2017) 355–364.
[31] K. Moreau, M. Coen, A.X. Zhang, F. Pachl, M.P. Castaldi, G. Dahl, H. Boyd, C. Scott, P. Newham, Proteolysis-targeting chimeras in drug development: a safety perspective, Br. J. Pharmacol. 177 (8) (2020) 1709–1718.
[32] D. Papadopoulos, L. Uhl, S.A. Ha, M. Eilers, Beyond gene expression: how MYC relieves transcription stress, Trends Cancer. 9 (10) (2023) 805–816.
[33] P. Sharma, N. Kaushal, L.R. Saleth, S. Ghavami, S. Dhingra, P. Kaur, Oxidative stress-induced apoptosis and autophagy: balancing the contrary forces in spermatogenesis, Biochim. Biophys. Acta Mol. basis Dis. 1869 (6) (2023) 166742.

[34] E.L. Weisberg, N.J. Schauer, J. Yang, I. Lamberto, L. Doherty, S. Bhatt, A. Nonami, C. Meng, A. Letai, R. Wright, H. Tiv, P.C. Gokhale, M.S. Ritorto, V. De Cesare, M. Trost, A. Christodoulou, A. Christie, D.M. Weinstock, S. Adamia, R. Stone, D. Chauhan, K.C. Anderson, H.S. Seo, S. Dhe-Paganon, M. Sattler, N.S. Gray, J. D. Griffin, S.J. Buhrlage, Inhibition of USP10 induces degradation of oncogenic FLT3, Nat. Chem. Biol. 13 (12) (2017) 1207–1215.
[35] M. Ito, Y. Fujita, A. Shinohara, Positive and negative regulators of RAD51/DMC1 in homologous recombination and DNA replication, DNA Repair (Amst) 134 (2024) 103613.
[36] K.S. Prabhu, S. Kuttikrishnan, N. Ahmad, U. Habeeba, Z. Mariyam, M. Suleman, A. A. Bhat, S. Uddin, H2AX: a key player in DNA damage response and a promising target for cancer therapy, Biomed. Pharmacother. 175 (2024) 116663.
[37] V. Wachholz, A.M. Mustafa, Y. Zeyn, S.J. Henninger, M. Beyer, M. Dzulko, A. Piee-Staffa, C. Brachetti, P.S. Haehnel, A. Sellmer, S. Mahboobi, T. Kindler, W. Brenner, T. Nikolova, O.H. Krämer, Inhibitors of class I HDACs and of FLT3 combine synergistically against leukemia cells with mutant FLT3, Arch. Toxicol. 96 (1) (2022) 177–193.
[38] R. Winkler, A.S. Magdefrau, E.M. Piskor, M. Kleemann, M. Beyer, K. Linke, L. Hansen, A.M. Schaffer, M.E. Hoffmann, S. Poepsel, F. Heyd, P. Beli, T. Möröy, S. Mahboobi, O.H. Krämer, C. Kosan, Targeting the MYC interaction network in B-cell lymphoma via histone deacetylase 6 inhibition, Oncogene 41 (40) (2022) 4560–4572.
[39] C. Boyault, Y. Zhang, S. Fritah, C. Caron, B. Gilquin, S.H. Kwon, C. Garrido, T. P. Yao, C. Vourc'h, P. Matthias, S. Khochbin, HDAC6 controls major cell response pathways to cytotoxic accumulation of protein aggregates, Genes Dev. 21 (17) (2007) 2172–2181.
[40] J. Jin, T. Meng, Y. Yu, S. Wu, C.C. Jiao, S. Song, Y.X. Li, Y. Zhang, Y.Y. Zhao, X. Li, Z. Wang, Y.F. Liu, R. Huang, J. Qin, Y. Chen, H. Cao, X. Tan, X. Ge, C. Jiang, J. Xue, J. Yuan, D. Wu, W. Wu, C.Z. Jiang, P. Wang, Human HDAC6 senses valine abundancy to regulate DNA damage, Nature 637 (8044) (2025) 215–223.
[41] D. Kovalovsky, S. Noonepalle, M. Suresh, D. Kumar, M. Berrigan, N. Gajendran, S. Upadhyay, A. Horvath, A. Kim, D. Quiceno-Torres, K. Musunuri, A. Villagra, The HDAC6 inhibitor AVS100 (SS208) induces a pro-inflammatory tumor microenvironment and potentiates immunotherapy, Sci. Adv. 10(46):eadp3687 (2024).
[42] L. Ma, K. Zhang, Z. Huang, Y. Guo, N. Liu, J. Chen, X. Wang, Y. Liu, M. Li, J. Li, C. Yang, S. Liu, G. Yang, Development of novel silicon-based hydrophobic tags (SiHyT) for targeted proteins degradation, J. Med. Chem. 67 (23) (2024) 21344–21363.
[43] G.E. Winter, Extrapolating lessons from targeted protein degradation to other proximity-inducing drugs, ACS Chem. Biol. 19 (10) (2024) 2089–2102.